reported in humans [1,2,5–8]. Here we report a BFPP patient carrying compound heterozygous mutations with a novel *GPR56* mutation, p.S36Q, and a previously reported mutation, p.R38Q. Additionally, we review previous reports and discuss the radiological and clinical features of BFPP patients.

2. Case report

The proband was a Japanese female born from non-consanguineous parents. She had normal prenatal and perinatal histories and normal head growth, but showed developmental delay within the first year of life. Complex partial seizures occurred at 2 months; carbamazepine was effective for the seizures. Since the age of two years, epileptic spasms in clusters have appeared and have been refractory to medications. Around the age of four years, she developed tonic seizures causing drop attacks, in addition to epileptic spasms.

The seizures persisted despite treatment with multiple antiepileptic drugs. Interictal electroencephalogram (EEG) showed generalized bursts of sharp waves and slow spike-wave discharges with anterior predominance (Fig. 1). Video-EEG monitoring (Grass Technology, West Warwick, RI, USA) at 6 years old revealed that she suffered from frequent atypical absence seizures and tonic seizures. She was diagnosed with Lennox–Gastaut syndrome by specific EEG features and seizures. At this age, she had moderate to severe developmental delay (developmental quotient = DQ: 33). She was unable to walk without help, and her speech was limited to a few isolated words. Neurologic examination revealed mild spasticity, hyperactive deep-tendon reflexes, poor coordination, and exotropia. She showed neither dysmorphic features nor other congenital anomalies.

Brain MRI at 6 years of age revealed bilateral polymicrogyria with an anterior to posterior gradient, in contrast to the relatively spared perisylvian regions, patchy signal change in the bilateral white matter, hypoplastic pons, and multiple small cysts in the corpus callosum (Fig. 2).

2.1. Mutation analysis

DNA was extracted from peripheral blood leukocytes obtained from the patient and her parents using standard methods, and after obtaining informed consent from the parents. We performed a mutation screening of for all coding exons and flanking introns of *GPR56* using the high-resolution melt analysis (HRM) or capillary sequencing. PCR samples showing an aberrant melting curve pattern were sequenced. PCR primers and conditions are available on request.

Mutation analysis revealed a compound heterozygous mutation in exon 2 of*GPR56,* (c.107G>A and c.113G>A), (which presumably leads to amino acid changes), (p.S36N and p.R38Q, respectively) in the extracellular N-terminus of the protein. Her father was heterozygous for the p.S36N mutation, and her mother carried the p.R38Q mutation, which indicates an autosomal recessive inheritance (Fig. 3). Both changes were not found in one individual among 80 Japanese controls.

3. Discussion

BFPP is an autosomal recessive polymicrogyria syndrome, which was frequently underdiagnosed before genetic testing and high-resolution neuroimaging were available.

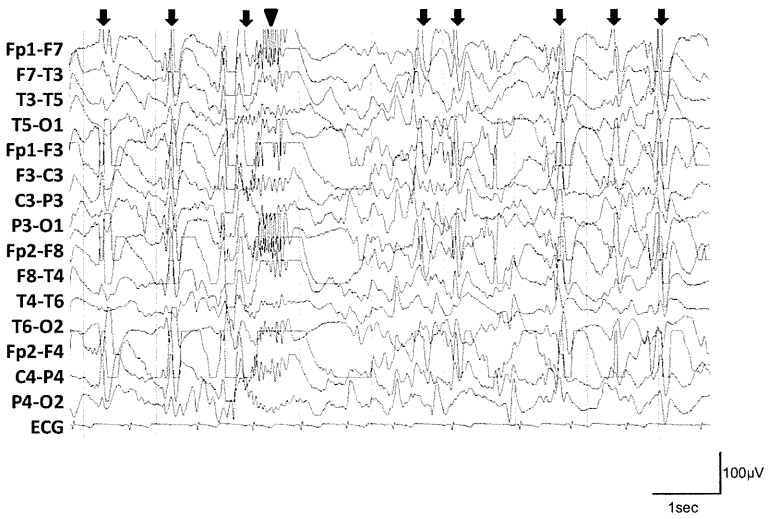

Fig. 1. Electroencephalography (EEG) finding. Generalized bursts of sharp waves (arrow head) and slow spike–wave discharges (arrows) with anterior predominance were seen during sleep.

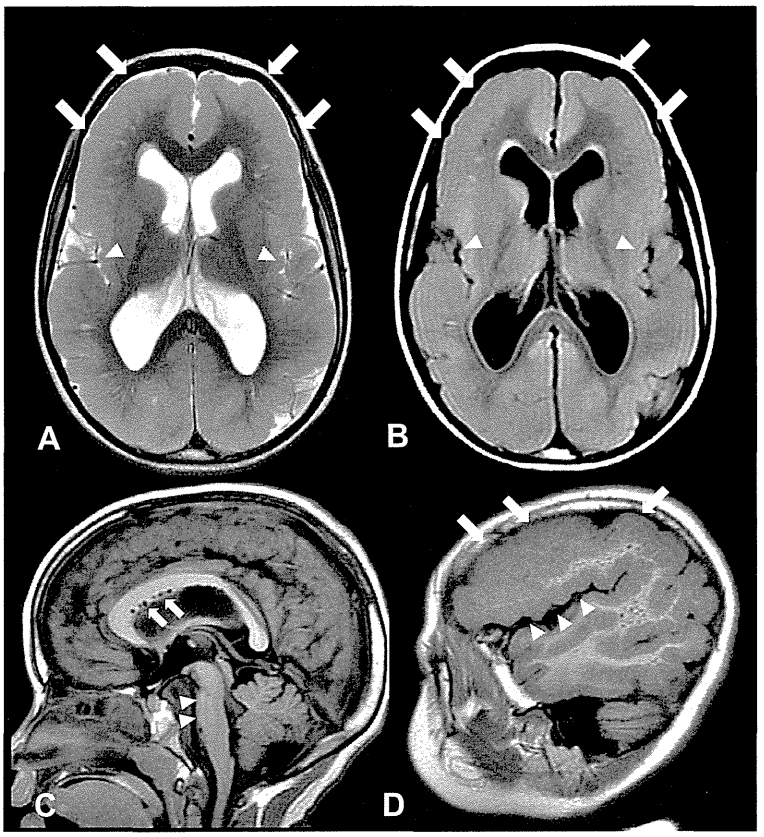

Fig. 2. Neuroimaging. Axial T2WI (A) and FLAIR (B) images demonstrate bilaterally symmetric thick cortex and irregular gyri compatible to polymicrogyria with anterior to posterior gradient (arrows) and, patchy high signals on both T2WI and FLAIR in the frontal subcortical white matter. Note the less involved insular cortex (arrow heads). Sagittal T1WI (C) shows flat pontine basis (arrow heads) and small cystic lesions in the corpus callosum (arrows). Sagittal T1WI (D) shows bilateral polymicrogyria with anterior to posterior gradient (arrows), in contrast with relatively spared perisylvian region (arrow heads).

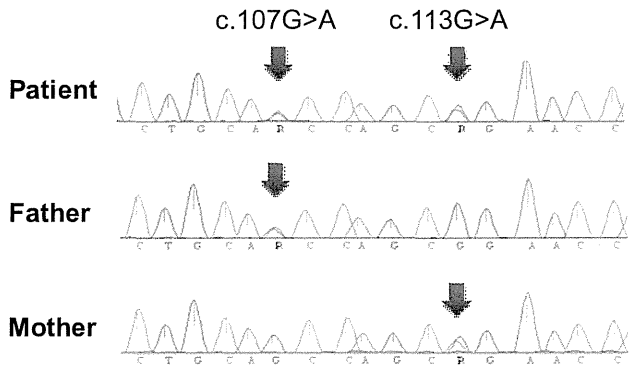

Fig. 3. Mutation analysis. Sequence chromatograms showing segregation of the compound heterozygous c.107G>A and c. 113G>A mutations in *GPR56* in the patient and her parents.

Piao, et al. [2] reported that the clinical phenotype of BFPP patients harboring *GPR56* mutations show considerable clinical homogeneity. This included five common clinical features and three typical MRI findings: (1) mental retardation of moderate to severe degree; (2) motor development delay; (3) seizures, most commonly symptomatic generalized epilepsy; (4) cerebellar signs, consisting of ataxia; (5) dysconjugate gaze, presenting variably as esotropia, nystagmus, exotropia, or strabismus; (6) bilateral polymicrogyria with anterior to posterior gradient; (7) bilateral patchy-white-matter signal changes without specific pattern; and (8) brain stem and cerebellar hypoplasia [1]. Thus, according to this description, our patient demonstrates the cardinal features of BFPP. Polymicrogyria typically has a predilection for the perisylvian cortex [9]. Our patient, however, shows less involvement of the perisylvian cortex, compared to the other regions where lesions were observed. Frontoparietal distribution of polymicrogyria is the most common feature of BFPP, but some patients show extensive distribution throughout the entire brain, as was observed with our patient [5,10]. Although other previous reports do not describe perisylvian cortex findings in detail, less involvement of perisylvian cortex might be a feature of BFPP caused by a GPR56 mutation.

Epilepsy is a common clinical problem in patients with BFPP caused by *GPR56* mutations [1,5–8,10]. Similar to our patient, four affected individuals from three families with BFPP caused by *GPR56* mutations had

Lennox–Gastaut syndrome [6]. Lennox–Gastaut syndrome manifestations can occur among patients with BFPP caused by GPR56 mutations.

Our patient had a compound heterozygous mutation of*GPR56* (p.S36N and p.R38Q), whereas other patients with BFPP have homozygous mutations of *GPR56* [1,2,5–8]. Both mutations are located in the ligand binding domain within the extracellular N-terminus of the protein, as was observed in the nine previously reported ligand binding domain mutations [1,2,5,6,8]. A homozygous p.R38Q mutation never has been reported with BFPP [1]. Moreover, a detailed analysis of the biochemical modifications by *GPR56* revealed that the disease-associated *GPR56* missense mutations in the tip of the N-terminal domain (p.R38Q) produced proteins with reduced intracellular trafficking and poor cell surface expression [11]. Similar to p.R38Q, p.S36N is another substitution and a novel mutation that locates a ligand binding domain within the extracellular N-terminus of the protein. Compound heterozygosity of these two mutations in the ligand binding domain could impair the subcellular trafficking of the GPR56 receptor, and reduce its cell surface expression, leading to BFPP.

Acknowledgments

This study was supported by the Health and Labour Sciences Research Grant from the Ministry of Health, Labour and Welfare of Japan (25140101) and a Grant-in-Aid for Scientific Research (C) from the Japan Society for the Promotion of Science (24591500) to M Kato. We thank Keiko Tanaka, Yamagata University, for providing technical assistance.

References

[1] Piao X, Chang BS, Bodell A, Woods K, Benzeev B, Topcu M, et al. Genotype–phenotype analysis of human frontoparietal polymicrogyria syndromes. Ann Neurol 2005;58:680–7.
[2] Piao X, Hill RS, Bodell A, Chang BS, Basel-Vanagaite L, Straussberg R, et al. G protein-coupled receptor-dependent development of human frontal cortex. Science 2004;303:2033–6.
[3] Stacey M, Lin HH, Gordon S, McKnight AJ. LNB-TM7, a group of seven-transmembrane proteins related to family-B G-protein-coupled receptors. Trends Biochem Sci 2000;25:284–9.
[4] Bjarnadóttir TK, Fredriksson R, Höglund PJ, Gloriam DE, Lagerström MC, Schiöth HB. The human and mouse repertoire of the adhesion family of G-protein-coupled receptors. Genomics 2004;84(1):23–33.
[5] Bahi-Buisson N, Poirier K, Boddaert N, Fallet-Bianco C, Specchio N, Bertini E, et al. GPR56-related bilateral frontoparietal polymicrogyria: further evidence for an overlap with the cobblestone complex. Brain 2010;133:3194–209.
[6] Parrini E, Ferrari AR, Dorn T, Walsh CA, Guerrini R. Bilateral frontoparietal polymicrogyria, Lennox–Gastaut syndrome, and GPR56 gene mutations. Epilepsia 2009;50:1344–53.
[7] Luo R, Yang HM, Jin Z, Halley DJ, Chang BS, MacPherson L, et al. A novel GPR56 mutation causes bilateral frontoparietal polymicrogyria. Pediatr Neurol 2011;45:49–53.
[8] Quattrocchi CC, Zanni G, Napolitano A, Longo D, Cordelli DM, et al. Conventional magnetic resonance imaging and diffusion tensor imaging studies in children with novel GPR56 mutations: further delineation of a cobblestone-like phenotype. Neurogenetics 2013;14:77–83.
[9] Leventer RJ, Jansen A, Pilz DT, Stoodley N, Marini C, Dubeau F, et al. Clinical and imaging heterogeneity of polymicrogyria: a study of 328 patients. Brain 2010;133:1415–27.
[10] Chang BS, Piao X, Bodell A, Basel-Vanagaite L, Straussberg R, Dobyns WB, et al. Bilateral frontoparietal polymicrogyria: clinical and radiological features in 10 families with linkage to chromosome 16. Ann Neurol 2003;53:596–606.
[11] Jin Z, Tietjen I, Bu L, Liu-Yesucevitz L, Gaur SK, Walsh CA, et al. Disease-associated mutations affect GPR56 protein trafficking and cell surface expression. Hum Mol Genet 2007;16:1972–85.

Pediatric Neurology 51 (2014) 441–443

Contents lists available at ScienceDirect

Pediatric Neurology

journal homepage: www.elsevier.com/locate/pnu

Clinical Observations

A Pediatric Case of Peripheral Polyneuropathy With IgM anti-GM1 Antibody Associated With a Group A Beta-Hemolytic *Streptococcus* Infection

Nobutsune Ishikawa MD [a,*], Yoshiyuki Kobayashi MD [a], Yuji Fujii MD [a], Makoto Samukawa MD [b], Susumu Kusunoki MD [b], Masao Kobayashi MD [a]

[a] *Department of Pediatrics, Hiroshima University Hospital, Hiroshima, Japan*
[b] *Department of Neurology, Kinki University School of Medicine, Osaka, Japan*

ABSTRACT

INTRODUCTION: Postinfectious peripheral neuropathy can be associated with various viral or bacterial infections. Group A beta-hemolytic *Streptococcus* infection can lead to neurological disorders, which involve predominantly the central nervous system, whereas peripheral neuropathy during childhood is rare. **PATIENT DESCRIPTION:** We describe a 12-year-old boy who presented with peripheral polyneuropathy associated with Group A beta-hemolytic *Streptococcus* infection. Anti-GM1 IgM was significantly elevated in his serum during the acute phase, which suggested that it was related with the pathophysiology in this patient. **CONCLUSION:** Group A beta-hemolytic *Streptococcus* infection may cause peripheral neuropathy via the autoimmune system and glycolipids.

Keywords: peripheral polyneuropathy, childhood, GABHS infection, antiglycolipids antibody

Pediatr Neurol 2014; 51: 441-443

Introduction

Group A beta-hemolytic *Streptococcus* (GABHS) infection has diverse subsequent complications. Central nervous system (CNS) signs occasionally follow GABHS infection,[1,2] whereas peripheral neuropathy related to GABHS infection during childhood has rarely been reported.[3]

Antiglycolipid antibodies play a crucial role in the pathomechanism of immune-mediated peripheral neuropathies. The IgG subtype is considered one of the main causes of these neuropathies,[4] whereas the IgM subtype has been reported in some.[5,6]

Here we describe a child with peripheral polyneuropathy related to GABHS infection with elevated serum IgM anti-GM1 antibody. It appears that GABHS infection caused autoimmune-mediated peripheral polyneuropathy via antiglycolipid antibodies.

Patient Description

This 12-year-old boy was referred for pain and tremor in his extremities. He had two febrile episodes, at an interval of 3 days, in which the fever disappeared within 1 day without treatment. Five days later, an additional febrile episode occurred with static and intention tremors of both arms. After this episode, he began to experience severe pain in all four extremities which was exaggerated by minimal touch. His mental state was altered, i.e., he became emotionally labile and tended to become excited and to begin crying easily. Four weeks after the onset of signs, he was admitted to our hospital.

On admission, there was a rash on both cheeks but no exanthema on other body surfaces. He was alert and conscious other than the mental changes described previously. His deep tendon reflexes were increased bilaterally, and mild muscle weakness was observed in the distal extremities. He had static and intention tremors of the extremities, predominantly on the left side; his hands and feet were pale and swollen with hyperhidrosis; and allodynia was observed predominantly at the distal extremities. His resting heart rate was accelerated at 110-120 bpm, but no arrhythmia or cardiac dysfunction was detected. Antinuclear, anti–double-stranded DNA, anti–single-stranded DNA, and anti–Jo-1 antibodies were negative. The serum creatine kinase level was within the

Article History:
Received January 10, 2014; Accepted in final form March 21, 2014

* Communications should be addressed to: Dr. Ishikawa; Department of Pediatrics, Hiroshima University Hospital, Kasumi 1-2-3, Minami-ku, Hiroshima 734-8551, Japan.
E-mail address: ishikan@hiroshima-u.ac.jp

0887-8994/$ - see front matter © 2014 Elsevier Inc. All rights reserved.
http://dx.doi.org/10.1016/j.pediatrneurol.2014.03.019

normal range. Although the anticytomegalovirus, Epstein-Barr virus, and antimycoplasma antibody titers did not suggest any recent infections, the antistreptolysin O (294 IU/mL [reference range, <199]) and antistreptokinase (×10,240 [reference range, <2560]) levels were markedly elevated, suggesting a recent GABHS infection. On serum antiglycolipids antibodies analysis, the IgM anti-GM1 antibody activity was elevated significantly (++; corrected optical density, 0.421). Examination of the cerebrospinal fluid did not reveal any specific findings, such as protein-cell dissociation, and head and spine magnetic resonance imaging did not reveal any lesions. A nerve conduction study did not reveal an evoked potential from sensory nerves, but there was a mild velocity decrease (26.7 m/second for the peroneal nerve and 37.4 m/second for the median nerve) and a compound muscle action potential decrease (0.35 mV for the peroneal nerve and 2.4 mV for the tibial nerve) in conjunction with temporal dispersion in the motor nerves. This suggests that a sensory-dominant sensorimotor polyneuropathy was present (Table). Consequently, a diagnosis of peripheral polyneuropathy associated with GABHS was made.

Oral prednisolone was initiated at 1 mg/kg/day and then reduced by 5 mg/1-2 weeks in conjunction with IV immunoglobulin therapy (1 g/kg/day) for three consecutive days. Gabapentin was administered to decrease the disproportionate pain and clarithromycin as antibiotic treatment for GABHS. The boy's emotional state, continuous pain, and allodynia improved 1 week after initiating treatment. Although a spiking fever persisted for 10 days and interstitial pneumonia was observed on computed tomography 3 weeks later, the blood examination and microbiological assay did not identify any causative abnormalities. The fever and interstitial pneumonia disappeared without specific therapy, and there was no recurrence. Three months after initiating treatment, the patient's signs improved and he returned to his normal school life. At that time, the antistreptolysin O and antistreptokinase titers were markedly reduced to 90 IU/mL and <1280, respectively. Five months later, the prednisolone was discontinued without symptom recurrence.

Discussion

Acute peripheral polyneuropathy during childhood commonly occurs as Guillain-Barré syndrome, which is differentiated into acute inflammatory demyelinating polyneuropathy, acute motor axonal neuropathy, and acute motor and sensory axonal polyneuropathy.[7] In our patient, sensory nerves were predominantly involved and the muscle weakness was mild, with no decrease in the deep tendon reflexes, which led to a diagnosis of sensory-dominant sensorimotor polyneuropathy. The electrophysiological study revealed severe axonal damage combined with demyelination. Diverse antiglycolipids antibodies play crucial roles in the pathophysiology of peripheral neuropathies. In this child, anti-GM1 IgM antibodies were significantly elevated, whereas all other antibodies were negative. The autoimmune process in Guillain-Barré patients is mediated by IgG subtype antiglycolipids antibodies,[4] whereas IgM subtypes contribute to other peripheral neuropathies.[5,6] GM1 is highly expressed in the axonal membranes of motor nerves and on the surface of Schwann cells.[8] Binding of GM1 antibodies to the axolemma at the nodes of Ranvier and Schwann cells might cause complement activation and ultimately disrupt sodium channel clusters, resulting in characteristic nerve conduction abnormalities such as nerve conduction slowing or block or decreased compound muscle action potential.[9,10] Although IgM anti-GM antibody is detected in multifocal motor neuropathy,[5] this child presented with sensory-dominant sensorimotor polyneuropathy, which revealed that IgM anti-GM1 antibody can contribute to sensory nerve neuropathy. A low IgM anti-GM1 antibody titer is present in normal adults,[11] whereas the markedly high level in our case suggests that this antibody affected his disease.

Our patient is unique because a GABHS infection was well-documented. There are rare reports of peripheral neuropathy related to streptococcal infection, although subsequent CNS involvement is occasionally described.[1,2] In this child, there was no direct evidence that the streptococcal infection caused the peripheral neuropathy, but the timing of the marked elevation of GABHS-related antibodies clearly corresponds to the onset of his disease. Therefore, we speculate that GABHS contributed to the onset of the peripheral neuropathy in this child. Systemic autoimmune pathology might also have led to the skin rash and altered mental status in this patient. Sydenham chorea is a well-recognized CNS complication of rheumatic fever. Most patients with Sydenham chorea exhibit behavioral change, such as emotional lability, distractibility, and anger, in addition to chorea.[12] It is assumed that there is specific and pathogenic autoimmune process affecting basal ganglia.[13] Other involuntary movements also occasionally follow a GABHS infection.[12] Our patient presented with a tremor, which might have been related to the GABHS infection.

This child's findings suggest that GABHS infections can cause a peripheral polyneuropathies via IgM anti-GM1

TABLE.
Nerve Conduction Study

Nerve Stimulated (Left Side)	Stimulation Site	Segment	Amplitude (mV)	Conduction Velocity (m/second)	F-wave Mean Latency (ms)
Median (M)	Elbow	Wrist-elbow	6.3	37.4	
	Wrist				28
Ulnar (M)	Elbow	Wrist-Elbow	7.5	56.6	
	Wrist				23.3
Peroneal (M)	Head of fibula	Ankle-head of fibula	0.35	26.7	
Tibial (M)	Popliteal	Ankle-popliteal	2.4	42.7	
	Ankle				45.9
Median (S)	Elbow	Wrist-elbow	Not evoked	Not evoked	
	Axilla	Elbow-axilla	Not evoked	Not evoked	
Ulnar (S)	Elbow	Wrist-elbow	Not evoked	Not evoked	
	Axilla	Elbow-axilla	Not evoked	Not evoked	

Abbreviations:
M = Motor nerve
S = Sensory nerve

antibody. Additional patients should be studied to determine the full manifestations of autoimmune-mediated peripheral polyneuropathy that occur during childhood.

The authors declare no potential conflicts of interest with respect to the authorship or publication of this article. The authors received no financial support for the research and authorship of this article.

References

1. Hachiya Y, Miyata R, Tanuma N, et al. Autoimmune neurological disorders associated with group-A beta-hemolytic streptococcal infection. *Brain Dev*. 2013;35:670-674.
2. Swedo SE, Leonard HL, Garvey M, et al. Pediatric autoimmune neuropsychiatric disorders associated with streptococcal infection: clinical description of the first 50 cases. *Am J Psychiatry*. 1998;155:264-271.
3. Munsat TL, Barnes JE. Relation of multiple cranial nerve dysfunction to the Guillain-Barré syndrome. *J Neurol Neurosurg Psychiatry*. 1965;28:115-120.
4. Schessl J, Koga M, Funakoshi K, et al. Prospective study on anti-ganglioside antibodies in childhood Guillain-Barré syndrome. *Arch Dis Child*. 2007;92:48-52.
5. Pestronk A, Choksi R. Multifocal motor neuropathy. Serum IgM anti-GM1 ganglioside antibodies in most patients detected using covalent linkage of GM1 to ELISA plates. *Neurology*. 1997;49:1289-1292.
6. Hughes BC, Allen D, Makowska A, et al. Pathogenesis of chronic inflammatory demyelinating polyradiculoneuropathy. *J Peripher Nerv Syst*. 2006;11:30-46.
7. Uncini A, Kuwabara S. Electrodiagnostic criteria for Guillain-Barré syndrome: A critical revision and need for an update. *Clin Neurophysiol*. 2012;123:1487-1495.
8. Willison HJ, Yuki N. Peripheral neuropathies and antiglycolipid antibodies. *Brain*. 2002;125:2591-2625.
9. Uetz-von Allmen E, Sturzenegger M, Rieben R, Rihs F, Frauenfelder A, Nydegger UE. Antiganglioside GM1 antibodies and their complement activating capacity in central and peripheral nervous system disorders and controls. *Eur Neurol*. 1998;39:103-110.
10. Susuki K, Rasband MN, Tohyama K, et al. Anti-GM1 antibodies cause complement-mediated disruption of sodium channel clusters in peripheral motor nerve fibers. *J Neurosci*. 2007;27:3956-3967.
11. Alaniz ME, Lardone RD, Yudowski SL, et al. Normally occurring human anti-GM1 immunoglobulin M antibodies and immune response to bacteria. *Infect Immun*. 2004;72:2148-2151.
12. Dale RC, Heyman I, Surtees RA, et al. Dyskinesias and associated psychiatric disorders following streptococcal infections. *Arch Dis Child*. 2004;89:604-610.
13. Dale RC, Brilot F. Autoimmune basal ganglia disorders. *J Child Neurol*. 2012;27:1470-1481.

Seizure 25 (2015) 136–140

Contents lists available at ScienceDirect

Seizure

journal homepage: www.elsevier.com/locate/yseiz

Increased interleukin-6 and high-sensitivity C-reactive protein levels in pediatric epilepsy patients with frequent, refractory generalized motor seizures

Nobustune Ishikawa *, Yoshiyuki Kobayashi, Yuji Fujii, Masao Kobayashi

Department of Pediatrics, Hiroshima University Hospital, Hiroshima, Japan

ARTICLE INFO

Article history:
Received 8 August 2014
Received in revised form 7 October 2014
Accepted 8 October 2014

Keywords:
High-sensitivity CRP
Intractable epilepsy
Generalized motor seizure
IL-6
PTX3
Chronic inflammation

ABSTRACT

Purpose: Recently, it was found that chronic inflammation contributes to the pathomechanism of diverse chronic diseases in various organs. There is accumulating evidence that inflammatory processes affect the pathophysiology of epilepsy. We investigated inflammatory markers to determine the chronic inflammatory process underlying the pathophysiology of intractable epilepsy presenting with frequent motor seizures in children.

Method: In total, 29 patients with epilepsy and 15 children as control subjects were enrolled. Patients were divided into the DS (daily generalized motor seizures) and the IS (intermittent seizures) groups. Blood levels of serum high-sensitivity C-reactive protein (hs-CRP), plasma pentraxin 3 (PTX3), serum tumor necrosis factor (TNF)-α, interleukin (IL)-6, and IL-β1 were evaluated in all participants.

Results: Hs-CRP levels were significantly higher in the DS group (0.149 ± 0.161 mg/dL) than in either the IS or control group (0.0156 ± 0.0136 and 0.0253 ± 0.0288 mg/dL, $p < 0.005$ and $p < 0.05$, respectively), while there was no significant difference between the IS and control groups. The IL-6 level was also significantly higher in the DS group (8.022 ± 0.161 pg/mL) than in either the IS or the control group (7.783 ± 0.0563 and 7.864 ± 0.072 pg/mL; $p < 0.005$ and $p < 0.05$, respectively). There were no significant differences in PTX3, TNF-α, or IL-1β levels.

Conclusion: Our results suggest that daily generalized motor seizures result in elevated IL-6 levels, leading to increased CRP. A systemic inflammatory response in intractable patients with frequent generalized motor seizures may affect their prognosis. We may need therapeutic strategies, including methods to control the inflammatory process, to treat intractable epilepsy.

1. Introduction:

Chronic inflammatory processes have been shown to play crucial roles in diverse chronic diseases, such as cardiovascular, respiratory, renal, and neurological diseases, in addition to the traditionally recognized 'inflammatory' diseases.[1–7] High-sensitivity C-reactive protein (hs-CRP) is a useful biomarker to detect chronic, subtle inflammation, which is not detected by conventional CRP values.[8,9] Pentraxin 3 (PTX3), a member of the pentraxin protein family, has been identified recently as a 'new' inflammatory marker. PTX3 is elevated mainly in cardiovascular diseases, although its elevation in some other chronic diseases has also been reported.[10–12]

Recently, accumulating evidence from experimental models and human studies has suggested that the pathophysiology of epilepsy also involves inflammatory process(es).[13–15] In previous studies, diverse cytokines have been evaluated in certain types of epilepsy,[16–21] while there have been few reports regarding other inflammatory markers. CRP levels were higher in partial secondarily generalized tonic–clonic seizures than in other types of partial seizures. There was a trend toward increased CRP concentrations in patients with recent tonic–clonic seizures and secondarily generalized seizures compared with control subjects.[22] PTX3 has been suggested to be synthesized in the brain after seizures and to exert a protective role against seizure-induced neurodegeneration.[23]

Intractable, frequent seizures at an early stage may be harmful in the brain development due to interference with developmental programs.[24,25] Intractable, frequent seizures at an early stage may be harmful in the brain development due to interference with developmental programs.[26,27]

* Corresponding author at: Department of Pediatrics, Hiroshima University Graduate School of Biomedical Sciences, Kasumi 1-2-3, Minami-ku, Hiroshima 734-8551, Japan. Tel.: +81 82 257 5212; fax: +81 82 257 5214.
E-mail address: ishikan@hiroshima-u.ac.jp (N. Ishikawa).

http://dx.doi.org/10.1016/j.seizure.2014.10.007
1059-1311/

We hypothesized that chronic inflammatory process(es) underlie the pathophysiology of intractable epilepsy presenting with frequent seizures in children. We considered that daily frequent motor seizures may cause more inflammation than do less frequent seizures. Thus, we investigated inflammatory markers, including hs-CRP, PTX3, tumor necrosis factor (TNF)-α, interleukin (IL)-6, and IL-β1, in the blood of patients with daily frequent seizures, particularly generalized motor seizures, compared with those with less frequent seizures and control subjects.

2. Materials and methods

2.1. Patients and controls

From June 2013 to February 2014, 29 patients with epilepsy (14 boys, 15 girls) and 15 children (7 boys, 8 girls) as control subjects were enrolled. The control group consisted of patients from Hiroshima University Hospital without epilepsy, fever, acute illness, or any other immune-mediated disorders. Epilepsy patients were diagnosed based on medical history and electroclinical (seizure semiology and EEG/video-EEG) and neuroimaging findings. They were divided into two groups: those who had daily generalized motor seizures (epileptic spasms, tonic seizures, secondarily generalized tonic–clonic seizures, and myoclonic seizures) and those who had intermittent (less than daily) seizures.

Patients in the daily seizure (DS) group ($n = 12$; 7 boys, 5 girls) had more than three seizures/day and those in the intermittent seizures (IS) group ($n = 17$; 7 boys, 10 girls) had less than one seizure/month. All patients in the DS group were monitored using a video-electroencephalogram (EEG) monitoring system for more than 24 h, and their seizure types and frequencies were confirmed by epilepsy specialists with clinical information. Video-EEG monitoring was performed using 21 scalp electrodes, which were placed according to the international "1–20" system, with electromyogram (EMG) sensors placed on the bilateral deltoid muscles.

The mean ages of the children in the DS, IS, and control groups were 4.54 ± 3.00, 6.44 ± 3.41, and 5.49 ± 4.37 years, respectively. No statistically significant differences in age, gender, body mass index, or treatment duration were observed among the three groups (Table 1, all $p > 0.05$). No patient in the DS or IS group had undergone any immune-related treatments, such as adrenocorticotropic hormone (ACTH), glucocorticoid, or immunoglobulin therapies, for at least 6 months before blood sampling.

This study was approved by the Hiroshima University Institutional Review Board. Written informed consent was obtained from the parents of each child.

2.2. Determination of serum hs-CRP, plasma PTX3, serum TNF-α, IL-6, and IL-1β levels

Serum and plasma samples were collected from the children who had no symptoms of infectious or inflammatory diseases. Peripheral venous blood was withdrawn from each subject and centrifuged (2000 × g, 20 min); serum or plasma was then isolated and stored at −80 °C for analysis within 6 h after collection. hs-CRP, PTX3, TNF-α, IL-6, and IL-1β concentrations were determined using commercially available kits. Hs-CRP concentrations were measured using a nephelometry method (N-Latex CRP II, Siemens Healthcare Diagnostics, Erlangen, Germany). PTX3 and TNF-α concentrations were each determined using quantitative sandwich enzyme immunoassay methods (Pentraxin 3 Quantikine for PTX3 and Quanti Glo Human TNF-α Chemiluminescent Immunoassay 2nd generation for TNF-α; R&D Systems, Minneapolis, MN, USA). IL-6 and IL-1β concentrations were measured by fluorescent bead-based immunoassays (Novex Singleplex Luminex Assay, Life Technologies, Carlsbad, CA, USA) based on the Luminex system (Luminex, Austin, TX, USA). All analyses were performed according to the manufacturers' instructions.

Table 1
Clinical characteristics of children in DS, IS, and control groups.

	DS group	IS group	Control group	
Age (years)	4.54 ± 2.63	6.4 ± 2.5	5.49 ± 3.61	*$p = 0.511$
Sex (male/subjects)	7/12	7/17	7/15	**$p = 0.692$
Body mass index	14.46 ± 3.44	15.72 ± 2.17	15.73 ± 3.15	*$p = 0.4658$
Duration (years)	3.86 ± 2.48	3.09 ± 1.86	N/A	***$p = 0.476$
Numbers of AEDs	2.58 ± 0.49	1.47 ± 0.61	N/A	***$p = 0.000421$

DS; daily seizures, IS; intermittent seizures, AEDs; antiepileptic drugs.
* Kruskal–Wallis test.
** Fisher's exact test.
*** Mann–Whitney *U* test, N/A; not applicable.

2.3. Statistical analyses

Data are shown as means ± standard deviation (SD), unless stated otherwise. Statistical analyses were performed using the statistical package 'R' (ver. 3.2.2; available at http://www.r-project.org). Numerical variables were compared using the Mann–Whitney *U*-test. A p value <0.05 was considered to indicate statistical significance. To examine differences between independent groups, the Kruskal–Wallis test and Fisher's exact test were used for categorical outcomes.

3. Results (Fig. 1)

Hs-CRP levels were significantly higher in the DS group (0.149 ± 0.161 mg/dL) than the IS and control groups (0.0156 ± 0.0136 and 0.0253 ± 0.0288 mg/dL; $p < 0.005$ and <0.05, respectively), whereas there was no significant difference between the IS and control groups. IL-6 levels were also significantly higher in the DS group (8.022 ± 0.161 pg/mL) than either the IS or control group (7.783 ± 0.0563 and 7.864 ± 0.072 pg/mL; $p < 0.005$ and < 0.05, respectively). The number of antiepileptic drugs (AEDs) used was significantly higher in the DS than IS group (2.583 vs. 1.471; $p < 0.001$). The PTX3 level was 0.72 ± 0.482 ng/mL in the DS group, 0.774 ± 0.463 ng/mL in the IS group, and 0.993 ± 0.539 ng/mL in the control group. Although the PTX3 level tended to be higher in the control group, no statistically significant difference was detected among the three groups. The TNF-α level was 1.245 ± 1.049 pg/mL in the DS group, 0.672 ± 0.537 pg/mL in the IS group, and 1.267 ± 1.084 pg/mL in the control group. The TNF-α level also tended to be higher in the control group, but no statistically significant difference was detected among the groups. The IL-1β level was 15.663 ± 0.0654 pg/mL in the DS group, 15.628 ± 0.037 pg/mL in the IS group, and 15.634 ± 0.0331 pg/mL in the control group. There were no statistically significant differences among the groups.

4. Discussion

Experimental evidence indicates significant roles for inflammatory and immune mediators in the initiation of seizures and epileptogenesis.[15–28] In particular, cytokines including IL-1β, IL-6, and TNF-α, and Toll-like receptor 4 have been shown to contribute to seizure generation and epileptogenesis.[28,29] In addition to experimental studies using animal models, human clinical studies have demonstrated alterations in the levels of IL-6 in samples from patients with epilepsy.[16] However, there are few data regarding TNF-α in patients with epilepsy, although seizures can induce the expression of TNF-α mRNA in the brains of animal models.[29] Experimental seizures were associated with post-ictal increases in IL-1β in the CNS, while no observable differences in IL-1β concentrations after seizure were demonstrated.[16,20,30] Our results

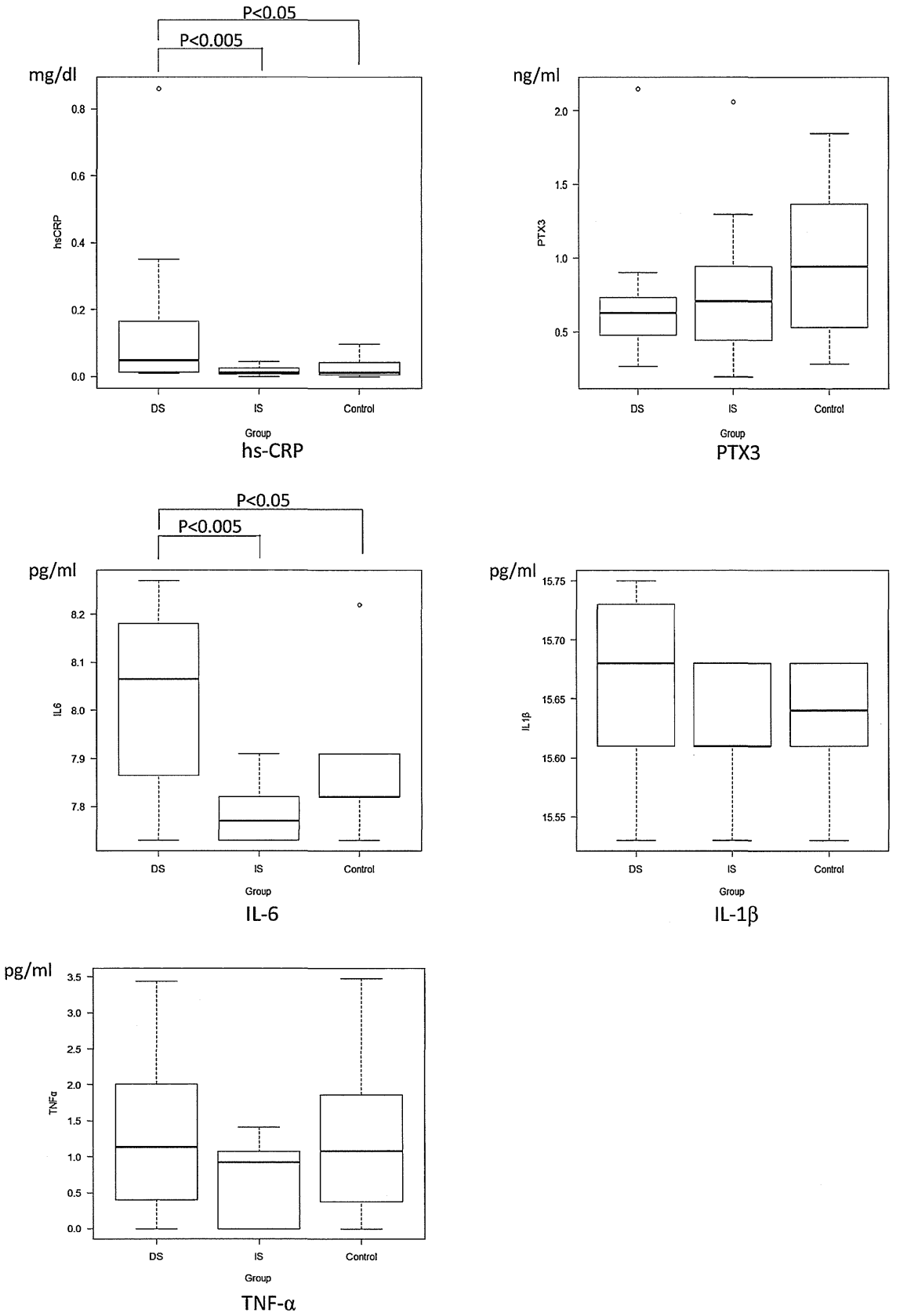

Fig. 1. Levels of inflammatory markers in the DS, IS, and control groups. The centerlines indicate medians, boxes indicate 25th–75th percentiles, and whiskers indicate the minimum and maximum values (white circles indicate outliers). DS, daily seizures, IS, intermittent seizures.

were similar to these previous findings. A rapid and transient post-ictal increase was seen in IL-6, which peaked at 12 h and remained elevated at 24 h.[16,17,20] The reason a significant increase in IL-6 was observed in the DS group may be because the multiple generalized motor seizures each day sustained the production of IL-6 before its degradation/turnover.

CRP, a member of the short pentraxins, is an established inflammatory marker produced by hepatocytes in response to inflammatory cytokines, such as IL-1, IL-6, and TNF-α, or to other stimulations.[10,31] Measurement of hs-CRP levels has recently been recognized as a method to detect chronic inflammation in patients with cardiovascular diseases,[1,2,32] stroke,[7] renal disease,[33] and neurodegeneration diseases.[5,34] PTX3 is a member of the long pentraxins produced in peripheral tissues and monocytic phagocytes in response to IL-1, TNF-α, and Toll-like receptor ligands.[35]

In this study, we showed that hs-CRP levels in patients with daily generalized motor seizures were significantly higher than those in other epilepsy patients or control subjects. These results may indicate that frequent motor seizures can cause chronic inflammation. Alapirtti et al[22]. suggested that secondarily generalized tonic–clonic seizures stimulated CRP even though other partial seizures did not. Peltola et al.[21] reported a significant correlation between plasma IL-6 and CRP concentrations in patients with recent tonic–clonic seizures. Our results suggest that daily generalized motor seizures provoked elevation of IL-6, leading to increased CRP levels.

Previous reports have shown that PTX3 is synthesized in the brain after seizures and may exert a protective role against seizure-induced neurodegeneration.[23] However, while plasma PTX3 has also been recognized as a biomarker of cardiovascular, renal disease, and systemic autoimmune diseases,[11,36–39] there is little information about its role as a plasma biomarker in patients with epilepsy. Although plasma PTX3 is useful for detecting vascular inflammation,[40] it may not be sensitive enough to provide inflammation about neuronal cells. We found no significant difference in PTX3 levels among the three groups. These results suggested that daily generalized motor seizures did not raise plasma PTX3 levels; however, there may be PTX3 production within the central nervous system.

It has been reported that AEDs may affect inflammatory markers. One study that examined markers for atherosclerosis risk in 195 epilepsy patients treated with AEDs showed higher CRP levels compared with controls.[41] Valproate is associated with lower CRP.[42] Significantly lower CRP values have been shown to associate with the use of lamotrigine and levetiracetam, and a trend for higher CRP values has been reported for patients on phenytoin and carbamazepine.[43] Long-term use of AEDs generally may result in low-grade systemic inflammation and increased oxidative stress.[41] In this study, there was no significant difference in treatment duration between the DS and IS groups. The number of AEDs used in the DS group was significantly greater than that in the IS group due to the refractory clinical course of the DS group. Yuen et al.[42] demonstrated no significant relationship between the number of AEDs taken and CRP. Thus, the higher levels of CRP in the DS group may be attributable to the frequent daily generalized motor seizures.

This study has certain limitations. Although the participants presented with no obvious inflammatory symptoms, CRP concentrations may fluctuate slightly over time with unnoticeable, subtle conditions, which may affect the validity of CRP levels.

Librizzi et al.[44] reported that seizures initiate brain inflammation in glia and promote blood–brain barrier damage independently of leukocytes or blood-borne inflammatory molecules, and brain inflammation can contribute to the duration and recurrence of seizures. In this study, we did not evaluate the intracellular conditions of neuronal cells. Systemic inflammatory responses in the intractable patients may have affected their prognoses. The impact of systemic inflammatory responses on generalized motor seizures in pediatric patients with epilepsy needs to be evaluated. The possible utility of anti-epileptic and anti-epileptogenesis therapies that target inflammation has been reported.[27,45] To treat intractable epilepsy, we may have to consider therapeutic strategies, including ways to control the inflammatory process too.

Conflict of interest statement

There is no possible conflict of interest (including financial and other relationship) for each author.

References

1. Gomez-Marcos MA, Recio-Rodriguez JI, Patino-Alonso MC, Agudo-Conde C, Gomez-Sanchez L, Rodriguez-Sanchez E, et al. Relationships between high-sensitive C-reactive protein and markers of arterial stiffness in hypertensive patients. Differences by sex. *BMC Cardiovasc Disord* 2012;**12**:37.
2. Assadpour Piranfar M. The correlation between high-sensitivity C-reactive protein (HSCRP) serum levels and severity of coronary atherosclerosis. *Int Cardiovasc Res J* 2014;**8**:6–8.
3. Deng ZC, Zhao P, Cao C, Sun SF, Zhao F, Lu CY, et al. C-Reactive protein as a prognostic marker in chronic obstructive pulmonary disease. *Exp Ther Med* 2014;**7**:443–6.
4. Firouzjahi A, Monadi M, Karimpoor F, Heidari B, Dankoob Y, Hajian-Tilaki K, et al. Serum C-reactive protein level and distribution in chronic obstructive pulmonary disease versus healthy controls: a case-control study from Iran. *Inflammation* 2013;**36**:1122–8.
5. Song IU, Chung SW, Kim JS, Lee KS. Association between high-sensitivity C-reactive protein and risk of early idiopathic Parkinson's disease. *Neurol Sci* 2011;**32**:31–4.
6. Impellizzeri D, Esposito E, Attley J, Cuzzocrea S. Targeting inflammation: new therapeutic approaches in chronic kidney disease (CKD). *Pharmacol Res* 2014;**81**:91–102.
7. VanGilder RL, Davidov DM, Stinehart KR, Huber JD, Turner RC, Wilson KS, et al. C-reactive protein and long-term ischemic stroke prognosis. *J Clin Neurosci* 2014;**21**:547–53.
8. Liuzzo G, Biasucci LM, Gallimore JR, Grillo RL, Rebuzzi AG, Pepys MB, et al. The prognostic value of C-reactive protein and serum amyloid a protein in severe unstable angina. *N Engl J Med* 1994;**331**:417–24.
9. Ridker PM. High-sensitivity C-reactive protein: potential adjunct for global risk assessment in the primary prevention of cardiovascular disease. *Circulation* 2001;**103**:1813–8.
10. Lech M, Rommele C, Anders HJ. Pentraxins in nephrology: C-reactive protein, serum amyloid P and pentraxin-3. *Nephrol Dial Transplant* 2013;**28**:803–11.
11. Ge W, Wang HL, Sun RP. Pentraxin 3 as a novel early biomarker for the prediction of Henoch–Schonlein purpura nephritis in children. *Eur J Pediatr* 2014;**173**:213–8.
12. Padeh S, Farzam N, Chayen G, Gerstein M, Berkun Y. Pentraxin 3 is a marker of early joint inflammation in patients with juvenile idiopathic arthritis. *Immunol Res* 2013;**56**:444–50.
13. Vezzani A, Granata T. Brain inflammation in epilepsy: experimental and clinical evidence. *Epilepsia* 2005;**46**:1724–43.
14. Vezzani A, Aronica E, Mazarati A, Pittman QJ. Epilepsy and brain inflammation. *Exp Neurol* 2013;**244**:11–21.
15. Vezzani A, Friedman A, Dingledine RJ. The role of inflammation in epileptogenesis. *Neuropharmacology* 2013;**69**:16–24.
16. Uludag IF, Bilgin S, Zorlu Y, Tuna G, Kirkali G. Interleukin-6, interleukin-1 beta and interleukin-1 receptor antagonist levels in epileptic seizures. *Seizure* 2013;**22**:457–61.
17. Peltola J, Palmio J, Korhonen L, Suhonen J, Miettinen A, Hurme M, et al. Interleukin-6 and interleukin-1 receptor antagonist in cerebrospinal fluid from patients with recent tonic–clonic seizures. *Epilepsy Res* 2000;**41**:205–11.
18. Yamanaka G, Kawashima H, Oana S, Ishida Y, Miyajima T, Kashiwagi Y, et al. Increased level of serum interleukin-1 receptor antagonist subsequent to resolution of clinical symptoms in patients with West syndrome. *J Neurol Sci* 2010;**298**:106–9.
19. Shiihara T, Miyashita M, Yoshizumi M, Watanabe M, Yamada Y, Kato M. Peripheral lymphocyte subset and serum cytokine profiles of patients with West syndrome. *Brain Dev* 2010;**32**:695–702.
20. Peltola J, Hurme M, Miettinen A, Keranen T. Elevated levels of interleukin-6 may occur in cerebrospinal fluid from patients with recent epileptic seizures. *Epilepsy Res* 1998;**31**:129–33.
21. Peltola J, Laaksonen J, Haapala AM, Hurme M, Rainesalo S, Keranen T. Indicators of inflammation after recent tonic–clonic epileptic seizures correlate with plasma interleukin-6 levels. *Seizure* 2002;**11**:44–6.
22. Alapirtti T, Waris M, Fallah M, Soilu-Hanninen M, Makinen R, Kharazmi E, et al. C-reactive protein and seizures in focal epilepsy: a video-electroencephalographic study. *Epilepsia* 2012;**53**:790–6.
23. Ravizza T, Moneta D, Bottazzi B, Peri G, Garlanda C, Hirsch E, et al. Dynamic induction of the long pentraxin PTX3 in the CNS after limbic seizures: evidence for a protective role in seizure-induced neurodegeneration. *Neuroscience* 2001;**105**:43–53.
24. Neill JC, Liu Z, Sarkisian M, Tandon P, Yang Y, Stafstrom CE, et al. Recurrent seizures in immature rats: effect on auditory and visual discrimination. *Brain Res Dev Brain Res* 1996;**95**:283–92.

25. Liu Z, Yang Y, Silveira DC, Sarkisian MR, Tandon P, Huang LT, et al. Consequences of recurrent seizures during early brain development. *Neuroscience* 1999;**92**:1443–54.
26. Chen YH, Kuo TT, Chu MT, Ma HI, Chiang YH, Huang EY. Postnatal systemic inflammation exacerbates impairment of hippocampal synaptic plasticity in an animal seizure model. *Neuroimmunomodulation* 2013;**20**:223–32.
27. Rojas A, Jiang J, Ganesh T, Yang MS, Lelutiu N, Gueorguieva P, et al. Cyclooxygenase-2 in epilepsy. *Epilepsia* 2014;**55**:17–25.
28. Friedman A, Dingledine R. Molecular cascades that mediate the influence of inflammation on epilepsy. *Epilepsia* 2011;**52**(Suppl. 3):33–9.
29. Li G, Bauer S, Nowak M, Norwood B, Tackenberg B, Rosenow F, et al. Cytokines and epilepsy. *Seizure* 2011;**20**:249–56.
30. Alapirtti T, Rinta S, Hulkkonen J, Makinen R, Keranen T, Peltola J. Interleukin-6, interleukin-1 receptor antagonist and interleukin-1beta production in patients with focal epilepsy: a video-EEG study. *J Neurol Sci* 2009;**280**: 94–7.
31. Volanakis JE. Human C-reactive protein: expression, structure, and function. *Mol Immunol* 2001;**38**:189–97.
32. Wasilewska A, Tenderenda E, Taranta-Janusz K, Zoch-Zwierz W. High-sensitivity C-reactive protein and mean platelet volume in paediatric hypertension. *Pediatr Nephrol* 2010;**25**:1519–27.
33. Almroth G, Lonn J, Uhlin F, Nayeri F, Brudin L, Andersson B, et al. Fibroblast growth factor 23, hepatocyte growth factor, interleukin-6, high-sensitivity C-reactive protein and soluble urokinase plasminogen activator receptor. Inflammation markers in chronic haemodialysis patients? *Scand J Immunol* 2013;**78**:285–90.
34. Engelhart MJ, Geerlings MI, Meijer J, Kiliaan A, Ruitenberg A, van Swieten JC, et al. Inflammatory proteins in plasma and the risk of dementia: the Rotterdam study. *Arch Neurol* 2004;**61**:668–72.
35. Bonacina F, Baragetti A, Catapano AL, Norata GD. Long pentraxin 3: experimental and clinical relevance in cardiovascular diseases. *Mediat Inflamm* 2013;**2013**: 725102.
36. Mantovani A, Valentino S, Gentile S, Inforzato A, Bottazzi B, Garlanda C. The long pentraxin PTX3: a paradigm for humoral pattern recognition molecules. *Ann N Y Acad Sci* 2013;**1285**:1–14.
37. Jenny NS, Blumenthal RS, Kronmal RA, Rotter JI, Siscovick DS, Psaty BM. Associations of pentraxin 3 with cardiovascular disease: the multi-ethnic study of atherosclerosis. *J Thromb Haemost* 2014;**12**:999–1005.
38. Kimura S, Inagaki H, Haraguchi G, Sugiyama T, Miyazaki T, Hatano Y, et al. Relationships of elevated systemic pentraxin-3 levels with high-risk coronary plaque components and impaired myocardial perfusion after percutaneous coronary intervention in patients with ST-elevation acute myocardial infarction. *Circ J* 2013;**78**:159–69.
39. Bevelacqua V, Libra M, Mazzarino MC, Gangemi P, Nicotra G, Curatolo S, et al. Long pentraxin 3: a marker of inflammation in untreated psoriatic patients. *Int J Mol Med* 2006;**18**:415–23.
40. Yasunaga T, Ikeda S, Koga S, Nakata T, Yoshida T, Masuda N, et al. Plasma pentraxin 3 is a more potent predictor of endothelial dysfunction than high-sensitive C-reactive protein. *Int Heart J* 2014;**55**:160–4.
41. Tan TY, Lu CH, Chuang HY, Lin TK, Liou CW, Chang WN, et al. Long-term antiepileptic drug therapy contributes to the acceleration of atherosclerosis. *Epilepsia* 2009;**50**:1579–86.
42. Yuen AW, Bell GS, Peacock JL, Koepp MM, Patsalos PN, Sander JW. Effects of AEDs on biomarkers in people with epilepsy: CRP, HbA1c and eGFR. *Epilepsy Res* 2010;**91**:187–92.
43. Mintzer S, Skidmore CT, Abidin CJ, Morales MC, Chervoneva I, Capuzzi DM, et al. Effects of antiepileptic drugs on lipids, homocysteine, and C-reactive protein. *Ann Neurol* 2009;**65**:448–56.
44. Librizzi L, Noe F, Vezzani A, de Curtis M, Ravizza T. Seizure-induced brain-borne inflammation sustains seizure recurrence and blood–brain barrier damage. *Ann Neurol* 2012;**72**:82–90.
45. Kwon YS, Pineda E, Auvin S, Shin D, Mazarati A, Sankar R. Neuroprotective and antiepileptogenic effects of combination of anti-inflammatory drugs in the immature brain. *J Neuroinflamm* 2013;**10**:30.

PLOS | ONE

Kawasaki Disease-Specific Molecules in the Sera Are Linked to Microbe-Associated Molecular Patterns in the Biofilms

Takeshi Kusuda[1☯], Yasutaka Nakashima[1☯], Kenji Murata[1], Shunsuke Kanno[1], Hisanori Nishio[1], Mitsumasa Saito[2], Tamami Tanaka[1], Kenichiro Yamamura[1], Yasunari Sakai[1], Hidetoshi Takada[1], Tomofumi Miyamoto[3], Yumi Mizuno[4], Kazunobu Ouchi[5], Kenji Waki[6], Toshiro Hara[1]*

1 Department of Pediatrics, Graduate School of Medical Sciences, Kyushu University, Fukuoka, Japan, **2** Department of Bacteriology, Graduate School of Medical Sciences, Kyushu University, Fukuoka, Japan, **3** Graduate School of Pharmaceutical Sciences, Kyushu University, Fukuoka, Japan, **4** Department of Pediatric Infectious Disease, Fukuoka Children's Hospital and Medical Center for Infectious Disease, Fukuoka, Japan, **5** Department of Pediatrics, Kawasaki Medical School Hospital, Okayama, Japan, **6** Department of Pediatrics, Kurashiki Central Hospital, Okayama, Japan

Abstract

Background: Kawasaki disease (KD) is a systemic vasculitis of unknown etiology. The innate immune system is involved in its pathophysiology at the acute phase. We have recently established a novel murine model of KD coronary arteritis by oral administration of a synthetic microbe-associated molecular pattern (MAMP). On the hypothesis that specific MAMPs exist in KD sera, we have searched them to identify KD-specific molecules and to assess the pathogenesis.

Methods: We performed liquid chromatography-mass spectrometry (LC-MS) analysis of fractionated serum samples from 117 patients with KD and 106 controls. Microbiological and LC-MS evaluation of biofilm samples were also performed.

Results: KD samples elicited proinflammatory cytokine responses from human coronary artery endothelial cells (HCAECs). By LC-MS analysis of KD serum samples collected at 3 different periods, we detected a variety of KD-specific molecules in the lipophilic fractions that showed distinct m/z and MS/MS fragmentation patterns in each cluster. Serum KD-specific molecules showed m/z and MS/MS fragmentation patterns almost identical to those of MAMPs obtained from the biofilms formed *in vitro* (common MAMPs from *Bacillus cereus*, *Yersinia pseudotuberculosis* and *Staphylococcus aureus*) at the 1st study period, and from the biofilms formed *in vivo* (common MAMPs from *Bacillus cereus*, *Bacillus subtilis/Bacillus cereus/Yersinia pseudotuberculosis* and *Staphylococcus aureus*) at the 2nd and 3rd periods. The biofilm extracts from *Bacillus cereus*, *Bacillus subtilis*, *Yersinia pseudotuberculosis* and *Staphylococcus aureus* also induced proinflammatory cytokines by HCAECs. By the experiments with IgG affinity chromatography, some of these serum KD-specific molecules bound to IgG.

Conclusions: We herein conclude that serum KD-specific molecules were mostly derived from biofilms and possessed molecular structures common to MAMPs from *Bacillus cereus, Bacillus subtilis, Yersinia pseudotuberculosis and Staphylococcus aureus*. Discovery of these KD-specific molecules might offer novel insight into the diagnosis and management of KD as well as its pathogenesis.

Citation: Kusuda T, Nakashima Y, Murata K, Kanno S, Nishio H, et al. (2014) Kawasaki Disease-Specific Molecules in the Sera Are Linked to Microbe-Associated Molecular Patterns in the Biofilms. PLoS ONE 9(11): e113054. doi:10.1371/journal.pone.0113054

Editor: Adam Driks, Loyola University Medical Center, United States of America

Received August 4, 2014; **Accepted** October 16, 2014; **Published** November 20, 2014

Data Availability: The authors confirm that all data underlying the findings are fully available without restriction. All relevant data are within the paper and its Supporting Information files.

Funding: This work was supported by grants (Grant A for Toshiro Hara [No. 22249043], Grant C for Hisanori Nishio [No. 22591183]) from the Japan Society for the Promotion of Science, the Health and Labour Science Research Grants (for Toshiro Hara) from the Japanese Ministry of Health, Labour and Welfare, and grants (for Takeshi Kusuda and Kenji Murata) from the Japan Therapeutic Study Group for Kawasaki Disease (JSGK). The funders had no role in study design, data collection and analysis, decision to publish, or preparation of the manuscript.

Competing Interests: The authors have declared that no competing interests exist.

* Email: harat@pediatr.med.kyushu-u.ac.jp

☯ These authors contributed equally to this work.

Introduction

The etiology of Kawasaki disease (KD) remains unknown, however, KD has long been considered to be caused by an infectious agent, because of its characteristics of the symptoms, age distribution, seasonality, occurrence of community outbreaks and epidemic cycles. On the other hand, no consistently recoverable agents, lack of person-to-person transmission or a common

contagious source, and paucity of case clusters in families, schools or nurseries are supportive of a non-infectious cause for KD [1–3]. Temporal clustering and marked seasonality in KD occurrence in Japan, Hawaii and San Diego also suggest a wind-borne environmental trigger for this disease [4].

KD is also characterized by marked elevations of serum levels of proinflammatory cytokines and chemokines [2] and the activation of the innate immune system [5–7]. We have established a novel murine model of KD coronary arteritis by oral administration of FK565, which functions as a synthetic microbe-associated molecular pattern (MAMP) and a ligand to one of the innate immune receptors, nucleotide-binding oligomerization domain-containing protein (NOD) 1 [8]. In this report, we performed liquid chromatography-mass spectrometry (LC-MS) analysis of KD sera to find out KD-specific molecules and demonstrated that serum KD-specific molecules were closely linked to MAMPs in the biofilms.

Materials and Methods

Study subjects

All patients enrolled in this study were admitted to Kyushu University Hospital, Fukuoka Children's Hospital and Medical Center for Infectious Diseases, Kawasaki Medical School Hospital or Kurashiki Central Hospital between June 2010 and March 2014. The study subjects consisted of 117 patients with KD (median age, 21 months; range 3–96 months; male/female, 65/52), 101 controls with other febrile illnesses (DC: median age, 16 months; range 0–121 months; male/female, 61/40), and 5 normal controls (NC: median age, 6 months; range 3–39 months; male/female, 1/4). A diagnosis of KD was made according to the Diagnostic Guidelines of KD [9]. The Ethical Committee of Kyushu University approved the study. Written informed consent was obtained from all guardians. The 1st study subjects (samples were collected mostly between July 2011 and February 2012) consisted of 43 patients with KD, 41 controls with DC (respiratory syncytial virus infection: $n=4$, influenza A virus infection: $n=7$, adenovirus infection: $n=2$, exanthema subitum: $n=5$, varicella: $n=2$, bacteremia: $n=2$, pneumonia: $n=6$, tonsillitis: $n=1$, lymphadenitis: $n=5$, cellulitis: $n=1$, urinary tract infection: $n=1$, gastritis: $n=5$), and 5 NC. The 2nd (mostly between May 2012 and July 2013) and 3rd (mostly between November 2013 and March 2014) study subjects consisted of 41 KD patients and 30 DC controls (respiratory syncytial virus infection: $n=8$, influenza A virus infection: $n=4$, adenovirus infection: $n=2$, exanthema subitum: $n=2$, herpetic stomatitis: $n=1$, pneumonia: $n=5$, bronchitis: $n=2$, upper respiratory infection: $n=1$, tonsillitis: $n=2$, deep neck abscess: $n=1$, acute otitis media: $n=1$, urinary tract infection: $n=1$), and 33 KD patients and 30 DC controls (respiratory syncytial virus infection: $n=8$, influenza A virus infection: $n=1$, adenovirus infection: $n=1$, pneumonia: $n=6$, bronchitis: $n=1$, upper respiratory infection: $n=4$, tonsillitis: $n=2$, lymphadenitis: $n=1$, sinusitis: $n=1$, acute otitis media: $n=1$, urinary tract infection: $n=2$, gastritis: $n=2$), respectively.

Sample collection

Blood samples were collected at the time of routine examinations before and after high-dose intravenous immunoglobulin (IVIG) therapy, and after resolution of symptoms. The sera were separated by centrifugation and stored at −30°C until the analysis.

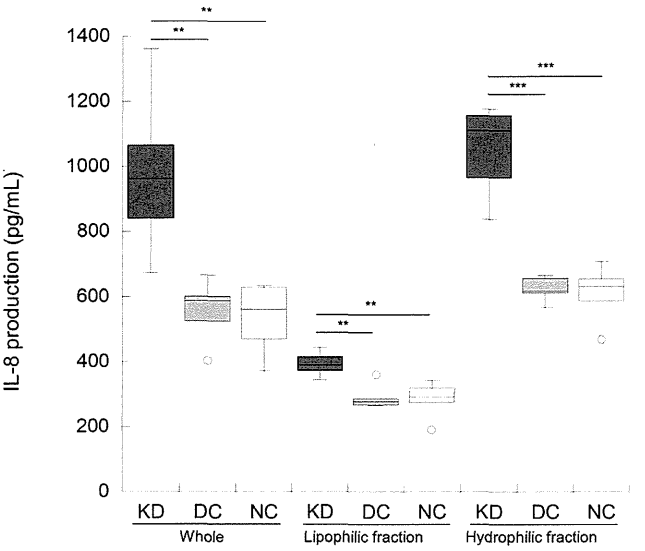

Figure 1. Whole and fractionated serum samples from KD patients induce cytokine production in HCAECs. The production of IL-8 by HCAECs was measured in triplicate after 24-hour stimulation with whole sera or lipophilic and hydrophilic fractions from KD patients (n = 6), DC controls (n = 5; pneumonia; n = 2, influenza A virus infection; n = 1, adenovirus infection; n = 1 and urinary tract infection; n = 1), or NC subjects (n = 5). Lipophilic and hydrophilic fractions were separated by ethyl acetate extraction. The bottom and top edges of the box plot correspond to the 25th and 75th percentiles, respectively. The horizontal line inside the box represents the median of the distribution. The whiskers indicate the 10th and 90th percentiles. $^{**}P<0.01$; $^{***}P<0.001$ (Welch's *t*-test).
doi:10.1371/journal.pone.0113054.g001

Routine bacterial cultures were performed with throat, tongue, nasal and rectal swabs. Biofilms from teeth, tongue, nasal cavity, or rectum (stool) were collected by cotton swabs or interdental brushes (for teeth). These swabs or brushes were suspended in double distilled water (ddH_2O) immediately and stored at −30°C until the analysis. Simultaneous collection of biofilm and serum samples was performed at 2nd ($n=12$, mostly October-December, 2012) and 3rd ($n=11$, mostly January-February, 2014) study periods.

Lipid extraction

Serum samples or other specimens were separated into lipophilic and hydrophilic fractions by Folch method [10] or ethyl acetate extraction [11,12]. As for Folch method [10], 100 μL of serum was acidified to pH5 with acetic acid and mixed with 2:1 chloroform-methanol mixture (v/v) to a final volume 300 μL. The mixture was shaken and centrifuged at 3000 rpm for 10 minutes, and the bottom lipophilic layer and upper hydrophilic layer were collected and evaporated. The lipophilic pellet was dissolved in 5 μL of chloroform, 5 μL of dimethyl sulfoxide (DMSO), and 40 μL of ddH_2O and hydrophilic pellet was in 50 μL of ddH_2O. As for ethyl acetate extraction [11,12], 100 μL of serum was mixed with the same volume of ethyl acetate. After centrifugation, the upper lipophilic layer including the interface and the bottom

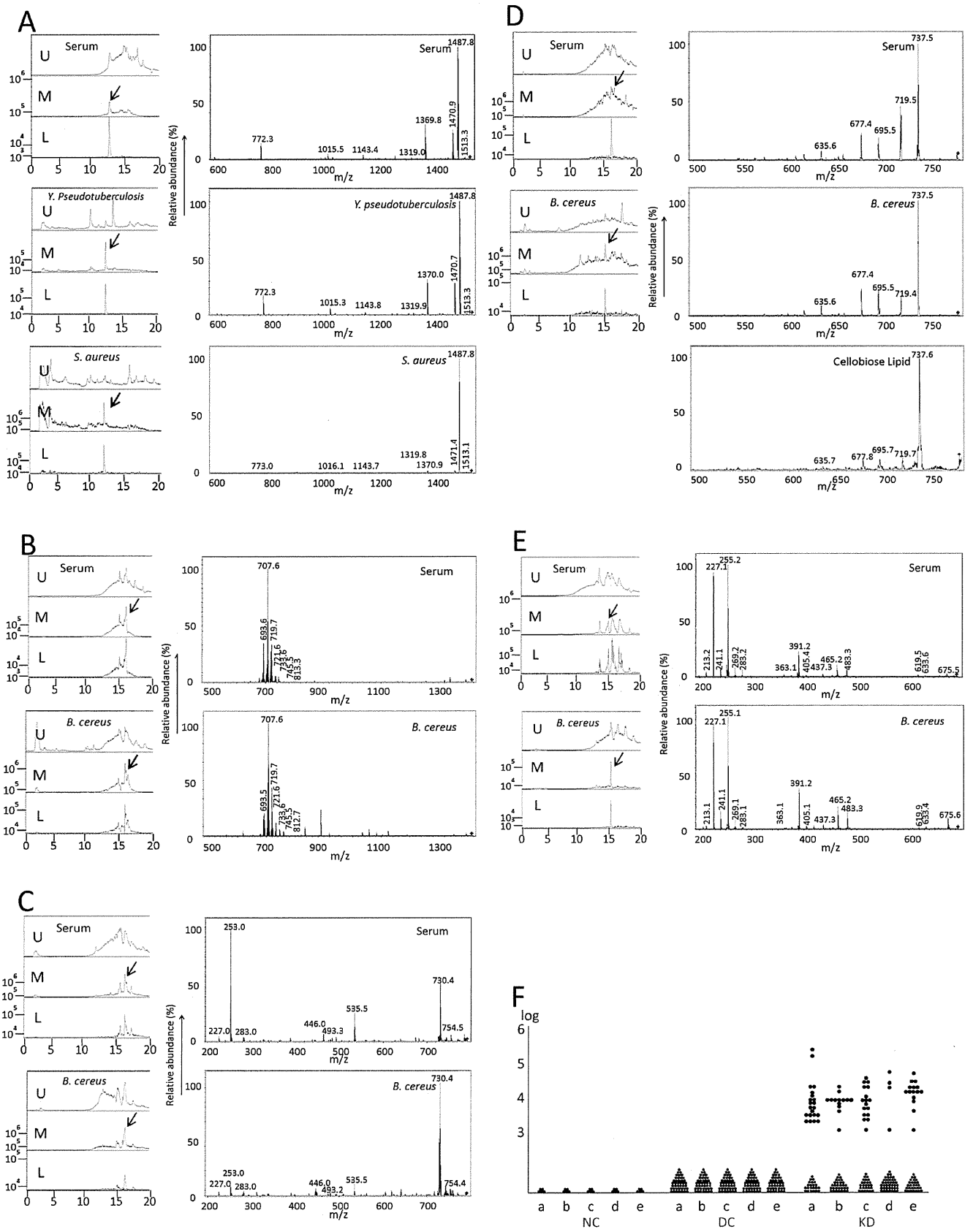
A
Serum
U
M
L
Y. Pseudotuberculosis
S. aureus
Relative abundance (%)
m/z
B
B. cereus
C
D
B. cereus
Cellobiose Lipid
E
F
log
NC
DC
KD

Figure 2. LC-MS chromatograms and MS/MS fragmentation patterns of serum KD-specific molecules at the 1st study period. A–E: Each left upper panel: LC-MS chromatograms of KD-specific molecules (A: m/z 1531.8, B: m/z 1414.3, C: m/z 790.9, D: m/z 779.8, and E: m/z 695.0), Each left lower panel: LC-MS chromatograms of biofilm extracts (or initial culture supernatants) from *Y. pseudotuberculosis* and *S. aureus* (A) and *B. cereus* (B–E). U: Total ion current chromatograms, M: Extracted-ion chromatograms at m/z 1500–1600 (A), m/z 1400–1500 (B), m/z 700–800 (C and D), and m/z 600–700 (E), L: Extracted-ion chromatograms at m/z 1531.8 (A), m/z 1414.3 (B), m/z 790.9 (C), m/z 779.8 (D), and m/z 695.0 (E). Arrows indicate peaks of target molecules. Each right upper panel: MS/MS fragmentation patterns of KD-specific molecules (A: m/z 1531.8, B: m/z 1414.3, C: m/z 790.9, D: m/z 779.8, and E: m/z 695.0), Each right lower panel: MS/MS fragmentation patterns of biofilm extracts (or initial culture supernatants) from *Y. pseudotuberculosis* and *S. aureus* (A) and *B. cereus* (B–E). As for the molecule at m/z 779.8, cellobiose lipid shows a MS/MS fragmentation pattern similar to that of KD sera (D, right lowest panel). The intensity is shown by relative abundance. F: The detection rates of each molecule in NC (N = 5), DC (N = 41) or KD (N = 43) sera are shown. Twenty-one (48.8%) of 43 are positive at m/z 1531.8 (a), 13 (30.2%) of 43 at m/z 1414.3 (b), 17 (39.5%) of 43 at m/z 790.9 (c), 4 (9.3%) of 43 at m/z 779.8 (d) and 15 (34.9%) of 43 at m/z 695.0 (e) when the intensity above 1×10^3 is considered to be significant. The overall detection rate was 76.7% (33 of 43). $P<0.0001$ (a, b, c and e); $P=0.0364$ (d) (Fisher's exact test).
doi:10.1371/journal.pone.0113054.g002

hydrophilic layer were transferred, evaporated, and dissolved in 50 μL of 20% methanol (lipophilic layers), and in 100 μL ddH_2O (hydrophilic layers) for cell stimulation, respectively. Since the human coronary artery endothelial cell (HCAEC)-stimulatory activities of KD serum samples were not stable after extraction with Folch method, we used ethyl acetate instead of chloroform. For LC-MS, lipophilic fractions were dissolved in 100% methanol. Other samples were also mixed with the same volumes of ethyl acetate, and centrifuged. Upper lipophilic layers including interfaces were collected, evaporated and dissolved in 100% methanol. To each sample, dibutyl hydroxytoluene was added at a final concentration of 1.0% as an antioxidant [13].

Cell stimulation

HCAECs (purchased from Lonza and no mycoplasma contamination) were cultured in EBM-2 medium with EGM-2MV (Lonza) in a 5% CO_2 incubator at 37°C. These cells, between passages 5 and 7, were suspended and seeded into 75 cm^2 flask. After passage, HCAECs were introduced in a 96 well plate (3×10^3 cells/well). On the following day, the medium was changed and the supernatants were collected for assay 24 hours after stimulation.

Cytokine assay

The concentrations of IL-8, IL-6, IL-1β, TNF-α, IL-12p70, and IL-10 in culture supernatants were measured by EC800 cell analyzer (Sony Corporation) with a BD Cytometric Bead Array human inflammation kit (BD Biosciences) [8]. We performed the experiments at least 3 times.

LC- MS analysis

Samples were analyzed by high performance liquid chromatography (HPLC, Agilent 1200 HPLC instrument, Agilent Technologies) on Dionex Acclaim surfactant column (3 μm, 120Å, 2.1×150 mm, DIONEX) and MS (Esquire 6000 electrospray ionization: ESI, Bruker Daltonics). The mobile phases were H_2O with 0.1% formic acid (eluent A) and acetonitril with 0.1% formic acid (eluent B). They were delivered at a flow rate of 0.2 ml/min and the column was operated at 25°C. The gradient was as follows: 0–3 min. 20% B, 3–12 min. 20–100% B, 12–70 min. 100% B. The injection volume to the system was fixed at 10 μl. The column eluent was connected to MS. The ESI-MS^n spectrum conditions were optimized in the negative-ion mode with the conditions as follows: nebulizer gas, 30.0 psi; drying gas, flow 8 l/min; dry temperature 330°C; high voltage (HV) capillary, 4500 V; HV end plate offset, −500 V; target ion trap, 30000; scan range 100–3000 m/z. The width for targeted precursor ions was set at 4 m/z.

Biofilm extraction from glass slides

After removing the medium, the culture tube and glass slides were washed once with PBS and vortexed in the presence of ethyl acetate. The ethyl acetate was transferred and evaporated, and the pellet was dissolved in 100% methanol. Details were described in Text S1 in File S1.

IgG affinity chromatography

Columns used included human polyclonal IgG-conjugated Sepharose 6 Fast (GE Healthcare Life Science), human IgG $F(ab')_2$ fragment-conjugated agarose (ROCKLAND), human IgG Fc fragment full length protein (Abcam)-coupled to cyanogen-bromide (CNBr) Sepharose 4B (GE Healthcare Life Science), mouse monoclonal IgG against a specific antigen (Myc-tag)-conjugated agarose (MBL), rabbit monoclonal IgG against a specific antigen (Phospho-Met (Tyr1234/1235) (D26) XP)-conjugated sepharose (Cell Signaling), and inactivated CNBr Sepharose 4B (GE Healthcare Life Science). Coupling to and inactivation of CNBr Sepharose 4B were performed according to the manufacturer's instructions. Each column was washed once with 10 volumes of PBS with 0.05% Tween20, and twice with 20 volumes of PBS. Biofilms extracts dissolved in PBS with 20% methanol or sera without dilution were applied to a column. After incubation for 30–60 minutes, the mixture was centrifuged and washed twice with PBS. Elution was performed with ethyl acetate. The ethyl acetate elutes were evaporated and the pellets were dissolved in 100% methanol. Inactivated CNBr Sepharose 4B was used as a control column. We performed the experiments at least 3 times.

Statistics

Data were analyzed by Welch's *t*-test and Fisher's exact test using a statistical software, JMP version 8.0 (SAS Institute), and *P*-values of <0.05 were considered to be statistically significant.

Results

Activation of HCAECs by KD sera *in vitro*

Since NOD1 ligand directly activates endothelial cells [8] and the expression of endothelial activation antigens was detected in KD skin biopsy specimens [14], HCAECs were employed for the

Table 1. The detection rates of serum KD-specific MAMPs at each study.

	1st KD study serum MAMPs						2nd KD study serum MAMPs					3rd KD study serum MAMPs		
	1531.8	**1414.3**	**790.9**	**779.8**	**695.0**		**1171.4**	**1169.4**	**906.8**	**695.0**		**667.4**	**619.4**	**409.3**
	% positive (positive number)						**% positive (positive number)**					**% positive (positive number)**		
1st KD study $n=43$	48.8 (21)	30.2 (13)	39.5 (17)	9.3 (4)	34.9 (15)		0.0 (0)	0.0 (0)	0.0 (0)	34.9 (15)		0.0 (0)	4.7 (2)	2.3 (1)
	76.7* (33)						34.9* (15)					7.0* (3)		
2nd KD study n=41						Pre	0.0 (0)	0.0 (0)	0.0 (0)	0.0 (0)				
	0.0 (0)	0.0 (0)	5.4 (2)	0.0 (0)	16.2 (6)	SBA period	16.7 (2)	16.7 (2)	33.3 (4)	50.0 (6)		0.0 (0)	0.0 (0)	0.0 (0)
						Post	0.0 (0)	0.0 (0)	10.0 (1)	0.0 (0)				
			16.2* (6)				SBA period: 83.3* (10)					0.0* (0)		
							Pre & Post: 3.4* (1)							
3rd KD study n=33											Pre	0.0 (0)	0.0 (0)	0.0 (0)
	0.0 (0)	0.0 (0)	0.0 (0)	0.0 (0)	0.0 (0)		0.0 (0)	0.0 (0)	16.1 (5)	0.0 (0)	SBA period	63.6 (7)	45.5 (5)	81.8 (9)
											Post	0.0 (0)	0.0 (0)	0.0 (0)
	0.0* (0)						16.1* (5)					SBA period: 90.9* (10)		
												Pre & Post: 0.0* (0)		

At the 2nd and 3rd studies, both *in vivo* biofilms and serum samples were simultaneously collected. *In vivo* biofilms samples were searched for MAMPs common to those in serum samples by LC-MS and MS/MS analyses. SBA: simultaneous biofilm analysis, *: overall % positive (overall positive numbers). DC samples at the 1st ($n=41$), 2nd ($n=30$) and 3rd ($n=30$) study periods were all negative for all KD MAMPs. The detection rates of KD-specific serum MAMPs between KD samples ($n=43$) and DC samples ($n=41$) at the 1st study showed statistically significant differences at m/z 1531.8, m/z 1414.3, m/z 790.9, m/z 695.0, and overall ($P<0.0001$), but not at m/z 779.8 ($P=0.1164$) by Fisher's exact test. The detection rates between SBA period KD samples ($n=12$) and DC samples ($n=30$) at the 2nd study showed statistically significant differences at m/z 906.8 ($P=0.0044$), m/z 695.0 ($P=0.0002$) and overall ($P<0.0001$), but not at m/z 1171.4 ($P=0.0767$) and m/z 1169.4 ($P=0.0767$). The detection rates between SBA period KD samples ($n=11$) and DC samples ($n=30$) at the 3rd study showed statistically significant differences at all 3 molecules and overall ($P<0.0001$).

doi:10.1371/journal.pone.0113054.t001

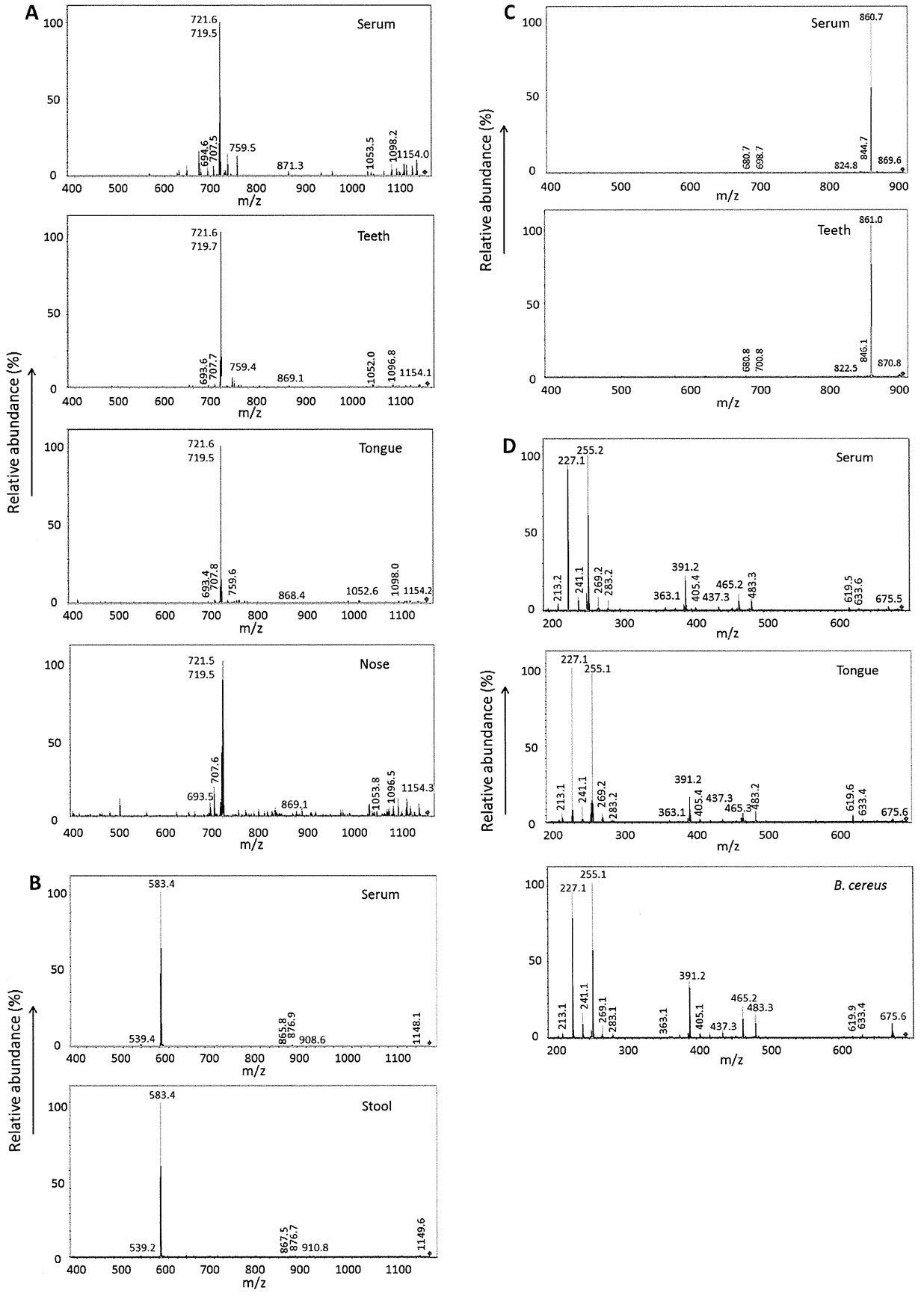
A
Serum
721.6
719.5
694.6
707.5
759.5
871.3
1053.5
1098.2
1154.0
Teeth
721.6
719.7
693.6
707.7
759.4
869.1
1052.0
1096.8
1154.1
Tongue
721.6
719.5
693.4
707.8
759.6
868.4
1052.6
1098.0
1154.2
Nose
721.5
719.5
693.5
707.6
869.1
1053.8
1096.5
1154.3
B
Serum
583.4
539.4
865.8
876.9
908.6
1148.1
Stool
583.4
539.2
867.5
876.7
910.8
1149.6
C
Serum
860.7
680.7
698.7
824.8
844.7
869.6
Teeth
861.0
680.8
700.8
822.5
846.1
870.8
D
Serum
255.2
227.1
213.2
241.1
269.2
283.2
363.1
391.2
405.4
437.3
465.2
483.3
619.5
633.6
675.5
Tongue
227.1
255.1
213.1
241.1
269.2
283.2
363.1
391.2
405.4
437.3
465.3
483.2
619.6
633.4
675.6
B. cereus
255.1
227.1
213.1
241.1
269.1
283.1
363.1
391.2
405.1
437.3
465.2
483.3
619.9
633.4
675.6
Relative abundance (%)
m/z

Figure 3. KD *in vivo* biofilms contain MAMPs common to serum KD-specific molecules (2nd study period). Extensive search for common molecules in the *in vivo* biofilms and sera from KD patients or DC controls revealed that 4 KD-specific molecules (m/z 1171.4, 1169.4, 906.8, and 695.0) showed similar MS/MS fragmentation patterns between the two in KD patients (Table S3 in File S1). A: The molecule at m/z 1171.4 was common in KD serum and biofilm extracts from teeth, tongue, or nose. B: The molecule at m/z 1169.4 was common in KD serum and stool biofilm extracts. C: The molecule at m/z 906.8 was common in KD serum and teeth biofilm extracts. D: The molecule at m/z 695.0 was common in KD serum and tongue biofilm extracts and *in vitro* biofilm extracts from *B. cereus*.
doi:10.1371/journal.pone.0113054.g003

search of such molecules as MAMPs in KD sera. KD samples induced significantly higher IL-8 production than DC and NC samples in whole sera. After separation into the lipophilic and hydrophilic fractions with ethyl acetate, KD samples elicited higher IL-8 production in each fraction (Figure 1). Similar results were obtained regarding IL-6 production. IL-6 and IL-8 levels in most of the tested sera from KD patients were under detection limits or negligible (data not shown). These results suggested that sera from KD patients contained molecules that stimulated HCAECs to produce IL-8 and IL-6. NOD1-stimulatory activity was also examined in whole and fractionated serum samples from KD, DC and NC, as described in Text S1 in File S1. However, no NOD1 activity was detected in any of these samples (data not shown).

Serum KD-specific molecules common to MAMPs from the *in vitro* biofilms

We explored serum KD-specific molecules in the lipophilic and hydrophilic fractions by LC-MS analysis, and found numerous KD-specific molecules in the lipophilic fractions in 10 KD patients of the 1st study period (data not shown). It has been reported that *Yersinia (Y.) pseudotuberculosis*-infected children sometimes develop KD [15,16]. Moreover, *Bacillus (B.) cereus* and *B. subtilis* were 2 major spore-forming bacteria isolated from KD patients (Table S1 in File S1), which might work as possible wind-borne environmental triggers for KD [4]. Therefore, to find out the MAMPs identical to serum KD-specific molecules, we initially analyzed culture supernatants (later biofilms) of *Y. pseudotuberculosis, B. cereus* and *B. subtilis* from KD patients by LC-MS. Five KD-specific molecules at m/z 1531.8, 1414.3, 790.9, 779.8, and 695.0 showed the m/z and MS/MS fragmentation patterns almost identical to those of the MAMPs from *Y. pseudotuberculosis* and *B. cereus* (Figure 2 and Figure S1 in File S1). The 5 serum KD-specific molecules were detected with 100% specificity and 9.3%–48.8% sensitivity. At least one of the 5 KD-specific molecules was detected in 33 (76.7%) out of 43 patients at the 1st study period (Figure 2, Table 1). All serum KD-specific molecules decreased after IVIG treatment (Figure S1F in File S1). By comparison with 5 authentic microbial glycolipids, only one molecule at m/z 779.8 showed a MS/MS fragmentation pattern similar to that of cellobiose lipid (Figure 2D).

As these microbes ceased production of these MAMPs after 1 or 2 passages, we investigated the optimal culture conditions (medium, temperature, duration, shaking, nutrition and biofilm formation) for the production of these MAMPs. We found that they produced these MAMPs reproducibly in the biofilm-forming conditions in the presence of lipid, especially butter (Figure S2 in File S1). We thus examined the culture supernatants and biofilm extracts from all the spore-forming microbes isolated from KD patients as well as additional microbes by LC-MS and MS/MS analyses. In addition to the 3 bacteria mentioned above, almost all KD-specific molecules were detected not in the culture supernatants but in the biofilm extracts. Although a KD-specific molecule at m/z 1531.8 was detected in biofilm extracts from several bacteria (Table S2 in File S1), *Y. pseudotuberculosis* and *Staphylococcus (S.) aureus* were isolated from KD patients. In addition, *B. cereus*-associated MAMPs were detected in the sera of KD patients from whom *B. cereus* was actually isolated (Figure 2, Figure S1 in File S1 and Table S1 in File S1).

Serum KD-specific molecules common to MAMPs from the *in vivo* biofilms

Although numerous KD-specific molecules were present in the lipid extracts from KD serum samples of the 2nd study period, the 5 KD-specific MAMPs observed at the 1st study period were no longer detected in the tested 10 samples. As the number of oligosaccharides, and the length, position, degree of saturation and configuration of the hydrophobic moieties in microbial glycolipids are known to change according to the environmental conditions and microbial origins [17,18], we examined lipid extracts from the *in vivo* biofilms in respective KD patients by LC-MS analysis. We detected 4 serum KD-specific molecules with MS/MS fragmentation patterns similar to one (m/z 695.0) of the 5 MAMPs at the 1st study period and 3 additional ones in the biofilms formed *in vivo* (teeth, tongue, nose and stool), respectively, in 10 (83.3%) out of 12 KD patients (Table S3 in File S1, Figure 3, Table 1). By the analysis of 20 microbial biofilm extracts and 5 authentic glycolipids, only one molecule at m/z 695.0 in tongue biofilms showed a MS/MS fragmentation pattern similar to that of a MAMP of *B. cereus* (Table S2 in File S1).

At the 3rd study period, we examined teeth and tongue biofilms and found 3 distinct KD-specific molecules with MS/MS fragmentation patterns similar to those from the *in vivo* biofilms in the respective KD patients by LC-MS and MS/MS analyses (Table S4 in File S1, Figure 4). Two of the 3 serum KD-specific molecules showed the MS/MS fragmentation patterns similar to a MAMP from *S. aureus*, and that from *B. subtilis*, *B. cereus* or *Y. pseudotuberculosis*, respectively. Actually, *B. subtilis* and *S. aureus* were detected from the patients. At least one of the 3 KD-specific MAMPs was detected in 10 (90.9%) out of 11 KD patients. The detection rates of KD-specific serum MAMPs at the 1st, 2nd and 3rd study periods are shown in Table 1. By LC-MS analysis, all the 106 control samples were negative for the 5, 4 and 3 KD-specific MAMPs detected at the 1st, 2nd and 3rd study periods, respectively.

IgG sepharose binds some serum KD-specific MAMPs

It has been reported that certain microbial glycolipids bound to various species of IgG [19,20]. Therefore, we checked IgG-binding activity of KD-specific MAMPs using various kinds of IgG affinity columns. LC-MS analysis of IgG sepharose-binding

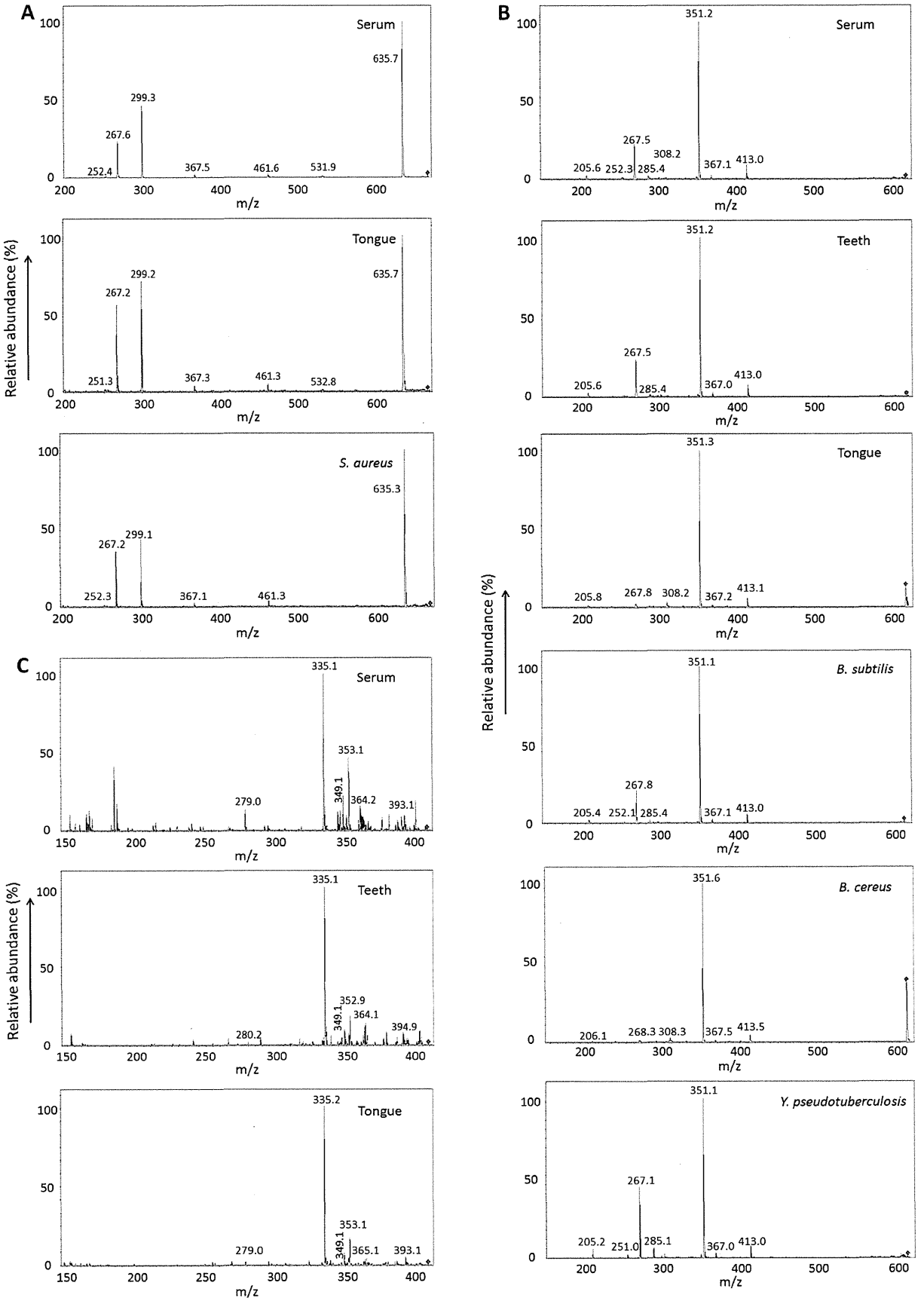
A
Serum
635.7
299.3
267.6
252.4
367.5
461.6
531.9
Tongue
635.7
299.2
267.2
251.3
367.3
461.3
532.8
S. aureus
635.3
299.1
267.2
252.3
367.1
461.3
B
Serum
351.2
267.5
308.2
205.6
252.3
285.4
367.1
413.0
Teeth
351.2
267.5
205.6
285.4
367.0
413.0
Tongue
351.3
205.8
267.8
308.2
367.2
413.1
B. subtilis
351.1
267.8
205.4
252.1
285.4
367.1
413.0
B. cereus
351.6
206.1
268.3
308.3
367.5
413.5
Y. pseudotuberculosis
351.1
267.1
205.2
251.0
285.1
367.0
413.0
C
Serum
335.1
353.1
279.0
349.1
364.2
393.1
Teeth
335.1
352.9
349.1
364.1
280.2
394.9
Tongue
335.2
353.1
279.0
349.1
365.1
393.1
Relative abundance (%)
m/z

Figure 4. KD *in vivo* biofilms contain MAMPs common to serum KD-specific molecules (3rd study period). Three serum KD-specific molecules (m/z 667.4, 619.4 and 409.3) at the 3rd study showed the same m/z with MS/MS fragmentation patterns similar to MAMPs from *in vivo* biofilm extracts (Table S4 in File S1) and *in vitro* bacterial biofilm extracts. A: The molecule at m/z 667.4 was common in KD serum, tongue biofilm extracts and *in vitro* biofilm extracts from *S. aureus*. B: The molecule at m/z 619.4 was common in KD serum, teeth and tongue biofilm extracts, and *in vitro* biofilm extracts from *B. subtilis, B. cereus* and *Y. pseudotuberculosis*. C: The molecule at m/z 409.3 was common in KD serum, and teeth and tongue biofilm extracts.
doi:10.1371/journal.pone.0113054.g004

molecules were conducted on KD and DC samples. Three KD-specific IgG sepharose-binding molecules were detected in KD sera of the 1st study period. One (m/z 1414.3) of the 5 serum KD-specific MAMPs (Figure 5A) and 2 other serum KD-specific MAMPs (m/z 745.6, 733.2) were detected in the IgG sepharose-binding fractions. The latter two were minor KD-specific MAMPs because they were detected in KD serum samples only after IgG sepharose purification. The MS/MS fragmentation patterns of the 3 molecules were similar to those of biofilm lipid extracts from *B.cereus*, while that of a molecule at m/z 733.2 also showed some similarity to that from *Y. pseudotuberculosis* (Figure S3 in File S1). To determine the IgG binding region of KD-specific MAMPs, polyclonal IgG, monoclonal IgG, $F(ab')_2$, and Fc affinity columns were employed. Serum KD-specific MAMPs bound to IgG mainly via Fab non antigen-binding regions (Figure 5B).

Studies on the *in vitro* biofilm MAMPs from various microbes

We investigated the stimulatory effects of extracts from culture supernatants or *in vitro* biofilms from various microbes on HCAECs. The biofilm extracts from *B. cereus* (9 out of 9 strains), *B. subtilis* (2 out of 5), *Y. pseudotuberculosis* (4 out of 4), *Pseudomonas (P.) aeruginosa* and *S. aureus* robustly induced the production of IL-8 and/or IL-6 by HCAECs, especially when microbes were cultured in the presence of sterilized butter (Figure 6). Biofilm extracts from *B. cereus*, *B. subtilis*, *Y. pseudotuberculosis*, *P. aeruginosa* and *S. aureus* were further fractionated by HPLC. In all of these 5 bacteria, HCAEC-stimulatory activity was observed in the same fractions (Figure 7). LC-MS analysis revealed that there were no common MAMPs in the fractions with high HCAEC-stimulatory activity among the biofilm extracts from *Y. pseudotuberculosis*, *B. cereus*, *B. subtilis*, *S. aureus* and *P. aeruginosa*.

Discussion

The present study showed that serum KD-specific molecules had distinct m/z and MS/MS fragmentation patterns in each temporal clustering of outbreaks. These findings are consistent with the fact that cases in each cluster share similar clinical features [21].

At the 1st study period, we detected 5 KD-specific molecules in patients' sera that were common to MAMPs from *in vitro* biofilms (4 from *B. cereus*, and 1 from *Y. pseudotuberculosis/S. aureus*). At the 2nd and 3rd study periods, we detected 4 and 3 serum KD-specific molecules in patients' sera, respectively, common to MAMPs from *in vivo* biofilms (1 from *B. cereus*, 1 from *B. subtilis/B. cereus/Y. pseudotuberculosis*, and 1 from *S. aureus*) in the respective KD patients. Although *Y. pseudotuberculosis* is sometimes involved in KD development [15,16], the detection rate of *Y. pseudotuberculosis*-type MAMPs was low in our study. Rather, *B. cereus*-type MAMPs were most frequently associated with KD, and indeed *B. cereus* itself was isolated from our patients. In addition, microbes producing *B. subtilis*-type and *S. aureus*-type MAMPs were also associated with KD.

B. cereus, *B. subtilis*, *Y. pseudotuberculosis*, *S. aureus*, and *P. aeruginosa* produced endothelial cell-activating MAMPs only in the biofilm-forming conditions, mostly in higher amounts in the presence of butter (Figure 6). Four of the 5 bacteria were isolated from our KD patients, and *P. aeruginosa* was associated with KD development [22] and isolated from the small intestine of KD patients [23].

The biofilm formation may be found in living tissues including teeth, tongue, respiratory tract, middle ears, and gastrointestinal tract [24]. In KD, specific MAMPs were detected in sera as well as in the *in vivo* biofilm extracts from various sites by LC-MS analysis. Several molecules common to both KD patients' *in vivo* biofilms and sera were not present in the *in vitro* biofilm extracts of a single microbe, probably because they were products from polymicrobial biofilms *in vivo* [25]. The transition from the planktonic state to the sessile state in the biofilm induces a radical change in the gene and protein expression in bacteria. The biofilm matrix, composed of polysaccharides, proteins, nucleic acids and lipids, is newly produced and secreted to form the immediate extracellular environment [26]. Indeed, bacterial biofilm products were reported to induce a distinct inflammatory response in human cells compared to their planktonic counterparts [27]. In our study, not culture supernatants but biofilm extracts induced cytokine production in human endothelial cells (Figure 6).

Bacillus species including *B. cereus* and *B. subtilis* are volatile spore-forming rods widely distributed in soil and air, and sometimes induce infections and intoxications [28,29]. The necessity of the biofilm and a certain environmental condition might explain why the presence of *Bacillus* species in control individuals does not induce KD by itself, and why other types of *Bacillus* species infections such as bacteremia and meningitis are not associated with KD development. In addition, just like KD [2], there is no person to person transmission in *Bacillus* species-associated human diseases such as food poisoning [28] and anthrax [30].

At least some serum KD-specific MAMPs bound to IgG mainly via Fab non antigen-binding regions, just like other microbial glycolipids that showed a high binding affinity to human IgG via Fab constant regions [19,20]. Therefore, it is likely that high-dose IVIGs work, at least in part, as a scavenger of such MAMPs from the blood stream, a previously unrecognized mechanism in KD [31,32].

The main limitations of our study were that the structural analysis of these KD-specific MAMPs was hampered by the instability of the lipophilic molecules after purification, and that